ISSN 1512-1232

A COMPOSITE FINGERPRINT TEMPLATE FROM MULTIPLE IMPRESSIONS CALLED FINGERPRINT MOSAICKING SCHEME

Srinivasa Kumar Devireddy
St.Mary's Women's Engineering College, Guntur, A.P.,India

Abstract

A fingerprint-based verification system has two distinct phases of operation: (i) the enrollment phase, during which multiple impressions of a fingerprint are acquired and stored in the database as templates, and (ii) the authentication phase, where the query image of a user is matched against the stored templates pertaining to that user (Fig. 1). The solid-state sensors that are being increasingly deployed in commercial applications, however, sense only a limited portion of the fingerprint pattern present in the tip of the finger. The amount of information that can be extracted from such partial prints is substantially lower compared to that which can be extracted from more elaborate prints sensed using an optical sensor or even inked prints. The average number of minutiae points extracted from a Digital Biometrics optical sensor (500 × 500 image at 500 dpi) is 45 compared to 25 minutiae obtained from a Veridicom sensor image (300 × 300 image at 500 dpi). This loss of information affects the matching performance of the verification system - the relatively small overlap between the template and query impressions results in fewer corresponding points and therefore, results in higher false rejects and/or higher false accepts (Fig. 2).

To deal with this problem, we have developed a fingerprint mosaicking scheme that constructs a composite fingerprint template using evidence accumulated from multiple impressions. A composite template reduces storage, decreases matching time and alleviates the quandary of selecting the "optimal" fingerprint template from a given set of impressions. In the proposed algorithm, two impressions (templates) of a finger are initially aligned using the corresponding minutiae points. This alignment is used by a modified version of the well-known iterative closest point algorithm (ICP) to compute a transformation matrix that defines the spatial relationship between the two impressions. The resulting transformation matrix is used in two ways: (a) the two template images are stitched together to generate a composite image. Minutiae points are then detected in this composite image; (b) the minutia sets obtained from each of the individual impressions are integrated to create a composite minutia set. Our experiments show that a composite template improves the performance of the fingerprint matching system by □ 4%.

1 Introduction

Typically, two types of representations are used to assess the similarity between a pair of fingerprints: (a) the global representation that examines the structure and flow of ridges over the entire print, and (b) the local representation, that exploits the position and orientation of certain singular points, called minutiae, that are present in the print (e.g., ridge endings and ridge bifurcations). By building a composite image, the amount of information available for these two types of representation increases. For example, the number of minutiae points used to represent a fingerprint may increase when minutiae information from two impressions of a finger are integrated. Similarly, the amount of ridge information available for global representation may increase as well. The challenge lies in accurately registering multiple impressions of the finger in order to extract more information. An accurate registration would aid in efficient mosaicking of the impressions.

ISSN 1512-1232

Figure 1: Fingerprint verification: Multiple impressions of the same finger are stored in the database as templates. The query image is matched against the components of the template to verify the claimed identity.

(a) Template Image (b) Query Image

Figure 2: Two impressions (300×300) of the same finger acquired using the Veridi-com sensor. The two impressions are observed to have very little overlap.

Registering fingerprint images, however, is a difficult problem for the following two reasons: (a) The ridges in a fingerprint image may have non-linear distortions due to the effect of pressing a convex elastic surface (the finger) on a flat surface (the sensor). Moreover, these distortions may be present only in certain regions of the sensed image due to the non-uniform pressure applied by the subject. (b) The presence of dirt deposits on the sensor or the finger can result in noisy or occluded images. It is rather difficult to register pairs of fingerprint images that are distorted differently or affected by noise. Ratha et al. [1] have developed a mosaicking scheme to integrate multiple snapshots of a fingerprint. The multiple snapshots are acquired as the user rolls the finger on the surface of the sensor and, therefore, a specific temporal order is imposed on the image frames when constructing the composite image. The authors examine 5 composition schemes that stack the grayscale images together and construct a composite mosaicked image, by associating a confidence value with every pixel. They evaluate the efficacy of these schemes by observing the area and quality (in terms of the number of valid minutiae points detected) of the composite image. Their experiments indicate that the mosaicked image has a substantially larger area and, consequently, more number of minutiae points are detected. It has to be noted that in their technique, successive impressions will have spatial proximity. But, in the case of dab fingerprint impressions obtained at different time instances, the parametric transformation

ISSN 1512-1232

between impressions is not known. This complicates the problem of mosaicking fingerprint images captured at different time instances.

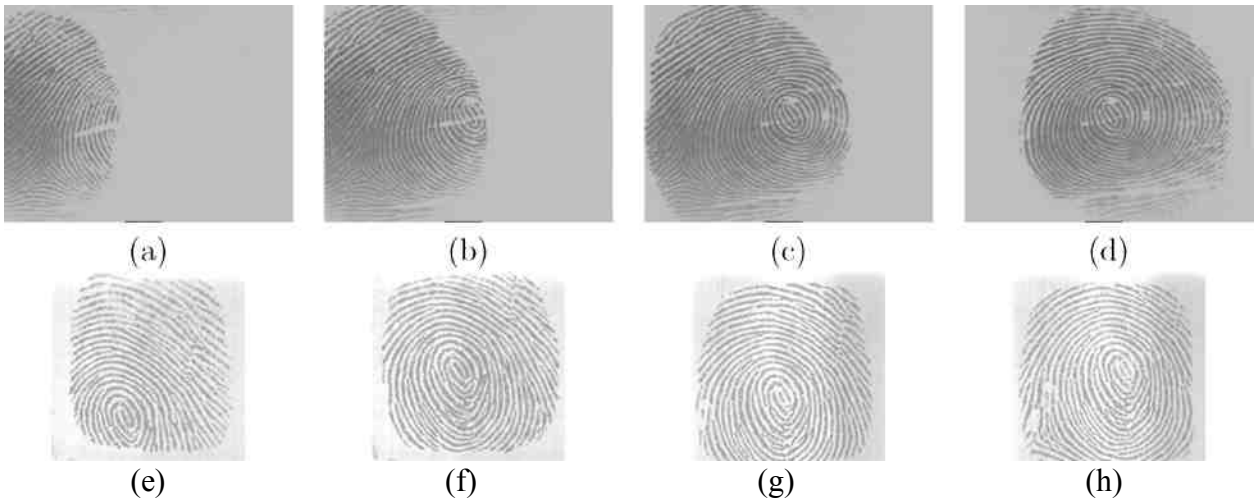

Figure 3: Rolled versus dab prints. (a) - (d): A sequence of 4 rolled fingerprint impressions obtained using the Digital Biometric sensor. Successive image frames are known to have spatial proximity. (e) - (h): Four impressions of a finger obtained at different time instances using a Veridicom sensor. The transformation between the impressions is not known.

We approach the problem of fingerprint mosaicking by treating the acquired fingerprint images as 3D surfaces. The rationale behind this is the observation that the imaging process involves pressing the 3D surface of the fingertip on a 2D flat surface. We assume that the resulting 2D intensity image indicates the pressure with which a user holds the finger against the surface of the sensor. Therefore, the intensity images may be treated as 3D range (surface) images.

In order to generate the transformation matrix defining the spatial relationship between two impressions, we employ the iterative closest point (ICP) algorithm that registers two 3D surface images when sufficient number of corresponding points are available between the two surfaces. The correspondences are used to compute an initial approximate alignment between the two surfaces; the ICP algorithm then attempts to find an optimal alignment such that the sum of distances between *control points* in one surface and the corresponding tangential planes in the other is minimized. Details of the algorithm is provided in the following section.

2 Fingerprint Image Registration

The problem of registering multiple 3D surfaces has received much attention in the literature [2][3]. A typical application of registration is 3D object model construction where multiple views of an object are integrated [4]. However, a variety of other applications exist for surface registration [5], including medical image analysis [6], terrain matching [7], etc.

A 3D surface registration algorithm seeks to find the best transformation T that relates two entities P and Q whose range images are given by R_P and R_Q, respectively. Thus the goal of a registration algorithm is to find T such that the following objective function, $D(R_P,R_Q)$, is minimized:

$$D(R_P, R_Q) = \sum_{p \in R_p} \left\| \mathrm{T}p - f\left(p\right) \right\|, \qquad (1)$$

where

$$f : P \to Q \mid \forall p \in R_p, f(p) \in R_Q$$

ISSN 1512-1232

The transformation, T, that is used to optimally align entities *P* and *Q,* usually depends upon the distortions present in the range images. Thus, T may be rigid, affine, polynomial, or elastic. For our application we assume T to be a rigid transformation. T can, therefore, be expressed as follows in homogeneous coordinates:

$$\mathrm{T} = \begin{bmatrix} \cos\alpha\cos\beta & \cos\alpha\sin\beta\sin\gamma - \sin\alpha\cos\gamma & \cos\alpha\sin\beta\cos\gamma + \sin\alpha\sin\gamma & t_x \\ \sin\alpha\cos\beta & \sin\alpha\sin\beta\sin\gamma + \cos\alpha\cos\gamma & \sin\alpha\sin\beta\cos\gamma - \cos\alpha\sin\gamma & t_y \\ -\sin\beta & \cos\beta\sin\gamma & \cos\beta\cos\gamma & t_z \\ 0 & 0 & 0 & 1 \end{bmatrix} \qquad (2)$$

Here α, β and γ are the rotation angles about the x, *y* and z axes, respectively, and t_x, t_y and t_z are the translation components along the three axes. Thus the matrix T has 6 independent parameters.In reality, the function f is not known and, therefore, the objective function in equation (1) has to be replaced by an evaluation function that assumes knowledge of a set of corresponding points in R_P and R_Q. Therefore, given a set of *N* pairs of corresponding points, $(p_i, q_i), p_i \in R_P, q_i \in R_Q$ and $i = 1... N$, one can try to minimize the evaluation function $e(R_P,R_Q)$:

$$e(R_P, R_Q) = \sum_{i=1}^{N} \left\| \mathrm{T}p_i - q_i \right\|^2 \qquad (3)$$

If the correspondences are not known, then it is not possible to register the images. Corresponding points are typically selected by extracting higher level features (e.g., edges, corners, texture, points of locally maximum curvature, etc.) from the two surfaces, and looking for similarities between the two sets of extracted features.

If the corresponding points are known, then the evaluation function shown in Equation (3) can be minimized by simply searching for the global minimum in the 6-dimensional parametric space using an iterative procedure. Such a procedure, however, does not guarantee convergence to a *global* minimum. To circumvent this problem, Chen and Medioni [8] assume that an initial approximate transformation, T_o, is known. A good starting approximation assures that the global minimum is reached quickly and surely. Equation (3) imposes a strict correspondence between points p_i and q_i. If the pair of points selected are incompatible (i.e., they are located on different surfaces in the two images), then an iterative procedure may converge very slowly. In order to deal with this issue, the ICP algorithm is used. This algorithm tries to minimize the distances between points in one image to geometric entities (as opposed to points) in the other. Chen and Medioni [8] attempt to minimize the distance of a point on one surface, to the tangential plane of the corresponding point in the other surface. Thus, they minimize

$$e^k(R_P, R_Q) = \sum_{i=1}^{N} d_s^2\left(\mathrm{T}^k p_i, s_j^k\right), \qquad (4)$$

where, d_s is the distance from the point to the plane, and S_j is the tangential plane corresponding to q_j in surface R_Q. Once an initial alignment is provided, the control points are automatically chosen by examining homogeneous regions in the two images.

An iterative procedure is adopted to converge to the global minimum (and hence the superscript *k* in the above equation). Since an approximate initial transformation matrix is known, convergence to the global minimum is assured, and since there is a relaxation in the condition of strict correspondence between points (equation (4)), convergence is faster.

ISSN 1512-1232

3 Fingerprint Mosaicking

We pose the fingerprint mosaicking problem as a 3D surface registration problem that can be solved using a modified ICP algorithm. The initial alignment of fingerprint images I_P and I_Q is obtained by extracting minutiae points from each individual image, and then comparing the two sets of minutiae points using an elastic point matching algorithm [12]. The comparison proceeds by first selecting a reference minutiae pair (one from each image), and then determining the number of corresponding minutiae pairs using the remaining sets of points in both the images. The reference pair that results in the maximum number of corresponding pairs is chosen. Let (p_Q,q_Q) be the reference minutiae pair and let $(p_1, q_1),\ldots (p_N, q_N)$ be the other corresponding minutiae pairs. Here, $p_i = (p_{x_i}, p_{y_i}, p_{z_i}, p_{\theta_i})$ and $q_i = (q_{x_i}, q_{y_i}, q_{z_i}, q_{\theta_i})$, where (x,y) are the spatial coordinates of the minutiae points, z is the intensity of the image at (x,y) and θ is the minutiae orientation. The initial transformation, T^0, is computed using Horn's method of unit quaternions [13] that operates on the (x, y, z) values. In this technique, the translation parameters in Equation (2) are computed using the centroid of the point sets $(p_{x_i}, p_{y_i}, p_{z_i})$ and $(q_{x_i}, q_{y_i}, q_{z_i})$, and the rotation components are computed using the cross-covariance matrix between the centroid-adjusted pairs of points.

3.1 Preprocessing the Fingerprint Image

Since the ICP algorithm uses distances from points to planes, it is very sensitive to rapid and abrupt changes in surface direction. Therefore, the fingerprint images are first median filtered using a 3×3 mask. This operation removes any undesirable "salt-and-pepper" noise that may be present in the valleys (furrows) of the fingerprint image (which may contribute to abrupt changes in the range image). The intensity values of the median filtered image are then scaled to a narrow range of values ([9, 10]) to ensure a fairly smooth change in surface direction in the corresponding range image of the fingerprints (Figure 4(b)).

3.2 Fingerprint Segmentation

The purpose of segmentation is to separate the foreground and background regions in the given intensity image. The foreground corresponds to those regions in the image that have valid fingerprint information (i.e., the ridges and valleys of the fingerprint), while the background represents those regions that do not have this information. It is useful to mask out the background of the images before registering the images using the ICP algorithm. This prevents the ICP algorithm from choosing control points in the background region (which is possible due to the homogeneity in intensity in these regions) and then attempting to align the images using these points. The algorithm to segment an image is as follows: (a) The preprocessed grayscale fingerprint image is converted to a binary image by examining the histogram of intensities and choosing a threshold. (b) An edge detection algorithm is applied to the binary image to get the outline of ridges. (c) Graham's convex hull algorithm [11] is used to generate a polygon that segments the fingerprint image (Figure 4(c)).

3.3 Fingerprint as a Range Image

The intensity values are directly used as range values. Therefore, the intensity value of the image at the planar coordinate (x,y) is treated as the range value at that location. We now have two range images R_P and R_Q, that are obtained from the corresponding intensity images I_P and I_Q, respectively. Figure 4(d) illustrates this mapping for a portion of the image in 4(c).

3.4 Registering Fingerprint Images

The two range images, R_P and R_Q, are now subject to the iterations of the ICP algorithm. At each iteration k, the transformation T^k that minimizes E^k in Equation (4) is chosen. The process is said to have converged when,

ISSN 1512-1232

$$\frac{\left|E^{k}-E^{k-1}\right|}{N}<\varepsilon,$$

where ϵ is some threshold, ϵ ≈ 0.

The final transformation matrix, $T^{solution}$, is used in the following two ways.

1. It is used to integrate the two individual images and create a composite image whose spatial extent is generally larger than the individual images. Minutiae points are then extracted from this larger image.

2. The minutiae sets from the individual images are augmented using $T^{solution}$.

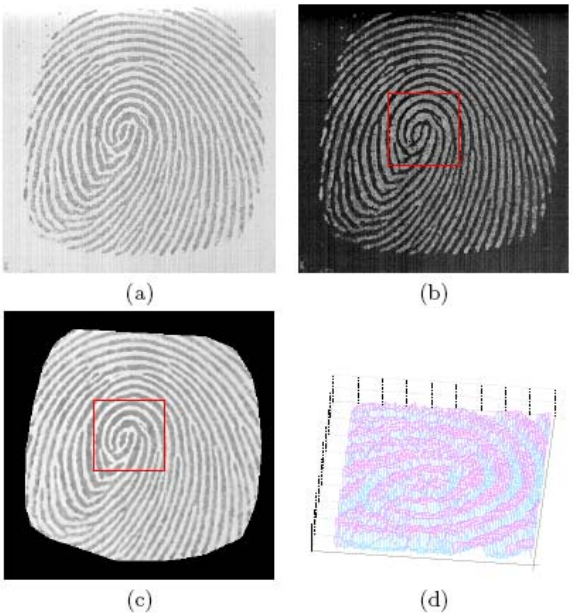

Figure 4: Mapping an intensity image to a range image. (a) The original intensity image. (b) The intensity image after median filtering and scaling. (c) The segmented intensity image. (d) The range image corresponding to the boxed region (rotated by □ 90°) in (c).

	Average Size	Average Number of Minutiae
Input Image	300 × 300	22
Mosaicked Image	336 × 332	30

Table 1: Increase in average image size and average number of detected minutiae as a result of mosaicking.

Mosaicked Images

The given intensity images I_P and I_Q are integrated into a new image I_R. Since $T^{solution}$ transforms I_P into I_Q, we compute the new spatial coordinates of every pixel I_P in I_R. We extract a new minutiae set (M_{R_1}) from this image using the algorithm described in [12] (see figure 5(e)). Note that the spatial extent of the composite image is generally larger than the individual

ISSN 1512-1232

images. Figure 6 shows the result of mosaicking on six different fingerprint pairs. Table 1 lists the increase in image size and the number of detected minutiae in the composite image.

The mosaicking procedure may sometimes result in poorly aligned images. This can happen when: (i) the segmentation of either of the images is erroneous, (ii) the images are noisy, or (iii) there are very few (< 5) corresponding points available to provide a valid initial alignment (Figure 7).

The intensity images I_P and I_Q are integrated into a new image I_R. Since $T_{solution}$ transforms I_P into I_Q, we compute the new spatial coordinate of every pixel I_P in I_R. We extract a new minutiae set (M_{R_1} from this composite image using the algorithm described in [12] (see figure 5).

Augmented Minutiae Sets

Let M_P refer to the minutiae set extracted from I_P and M_Q refer to the minutiae set extracted from I_Q. The composed minutiae set M_{R_2} is obtained by computing the (x, *y, θ)* parameter of each minutia in the composite image. The new (x, *y)* coordinates (i.e., the spatial coordinates) of the minutiae points (of the first image) is determined by simply multiplying the old coordinates with the transformation matrix (Figure 5f). The minutiae orientation, θ, is not recomputed.

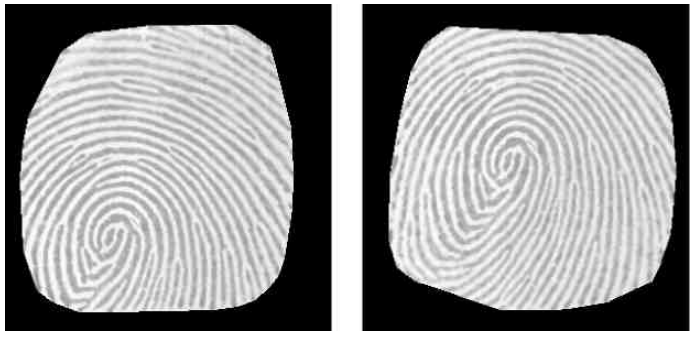

(a) (b)

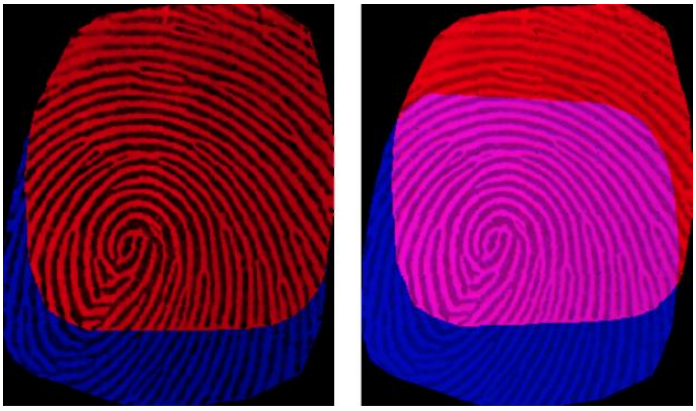

(c) (d)

ISSN 1512-1232

(e) (f)

Figure 5: Composite template construction: (a) First image after segmentation. (b) Second image after segmentation. (c) Initial alignment. (d) Final alignment. (e) Minutiae extracted from mosaicked images. (f) Composite minutiae set obtained by augmenting individual minutiae sets.

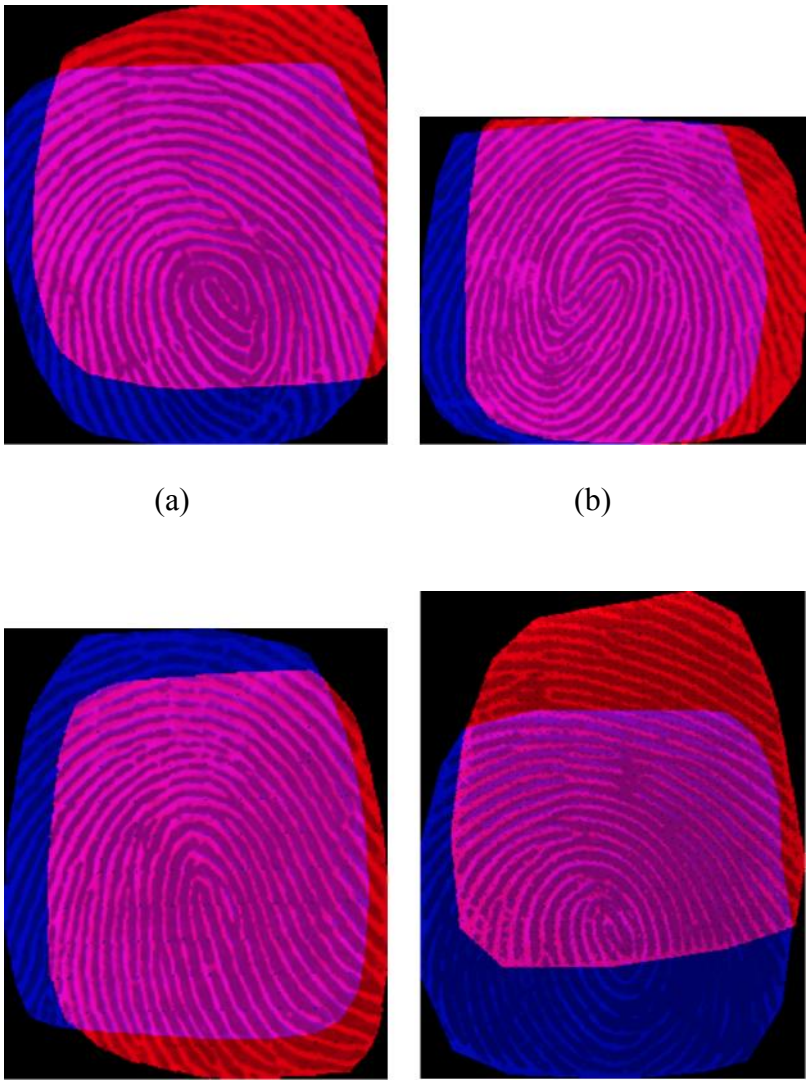

(a) (b)

(c) (d)

ISSN 1512-1232

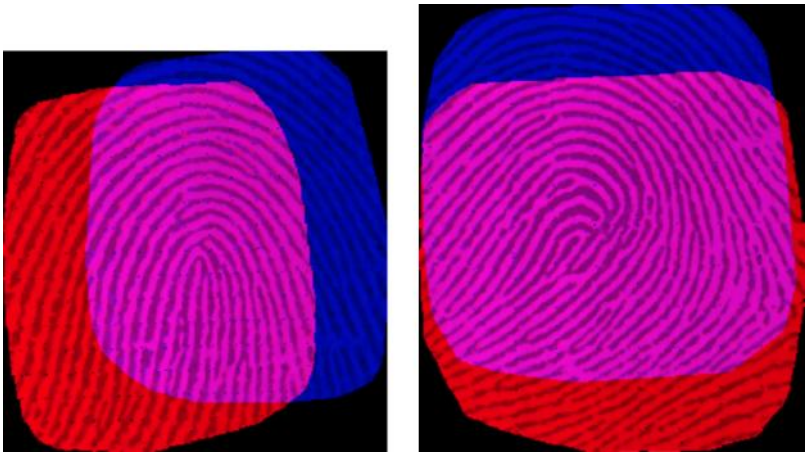

(e) (f)

Figure 6: The result of mosaicking six pairs of fingerprint impressions. The spatial extent of the mosaicked image is observed to be larger than that of the component images.

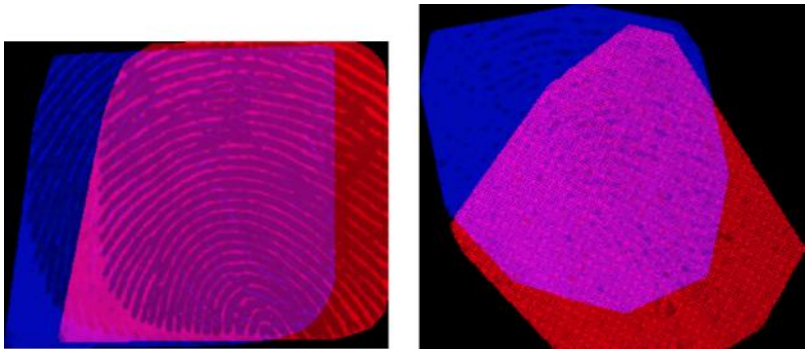

(a) (b)

Figure 7: Examples of poorly mosaicked image pairs. **Integrating Images**

4 Experimental Results

We have conducted the following experiments to validate the effectiveness of the transformation and integration described in section 3.4. We have two different techniques to obtain a composite minutiae set. The two minutiae sets are indicated by M_{R1} (obtained by extracting minutiae from the composite image), and M_{R2} (obtained by integrating individual minutiae sets). We treat these sets as template minutiae sets against which a query minutiae set can be matched.

Fingerprint images of 640 different fingers, corresponding to 160 different subjects, were acquired using the Veridicom sensor as described in the previous chapter. 4 different impressions of each of these fingers were obtained over two different sessions separated by a period of six weeks (2 impressions in each session). The two impressions acquired at the same session were used to construct the template minutiae set of a finger, while the other two impressions were used as query images during the test phase of the experiment. Thus, 640 pairs of images were used to construct the minutiae templates M_{R_1} and M_{R_2}, and the rest (1280) were used as query images.

Given a minutiae set M_U (of the query image I_U), and the template minutiae sets M_P, M_Q, M_{R_1} and M_{R_2}, we perform the following comparisons: (i) M_U with M_P, (ii)M_U with M_Q, (iii) M_U with

ISSN 1512-1232

M_{R_1}, and (iv) M_U with M_{R_2}. Thus we get a set of four scores corresponding to these comparisons. The ROC curves depicting the performance of these 4 different matchings are shown in figure 8. It is clear from these graphs that a composite template image results in improved matching performance. We further observe that a better matching performance is obtained by using M_{R_1} rather than M_{R_2}. This may be due to incorrect minutiae orientation in M_{R2}. Note that when augmenting the two minutiae sets, M_P and M_Q, no systematic technique is used to adjust the minutiae orientation in the composite minutiae template, M_{R_2}. While the use of M_{R_1} results in better matching performance, generating M_{R1} introduces several spurious minutiae that have to be carefully discarded. The spurious minutiae are a consequence of misalignment of the ridges present in the two individual impressions that are being integrated.

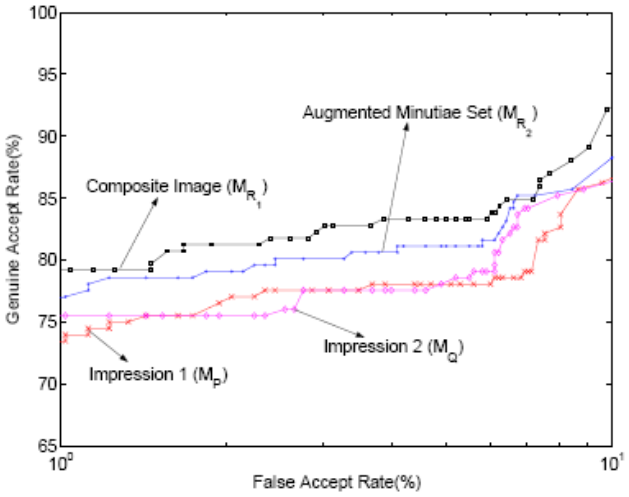

Figure 8: The ROC curves indicating improvement in matching performance after mosaicking templates. Utilizing the minutiae points that are extracted from the composite fingerprint image (M_{R1}) results in the best matching performance.

5 Conclusions

We have described a fingerprint template construction technique that integrates information available in two different impressions of the same finger. The method makes use of corresponding minutiae points to establish an initial approximate alignment, and a modified ICP algorithm to register the two impressions. The transformation matrix generated by the ICP algorithm is used to construct composite information from the individual impressions. Our experiments indicate that mosaicking the images together and then extracting the (template) minutiae set results in a better matching performance.The mosaicking scheme suggested here has been used to register two impressions of a finger. By repeated application of this procedure several impressions of a finger (> 2) may be integrated. Fingerprint mosaicking elegantly addresses the problem of partial fingerprint images and is, therefore, an essential component of a fingerprint recognition system.

ISSN 1512-1232

6 References

1. N. K. Ratha, J. H. Connell, and R. M. Bolle, "Image mosaicing for rolled fingerprint construction," in Proc. of 14th International Conference on Pattern Recognition, vol. 2, pp. 1651–1653, 1998.
2. P. J. Besl and N. D. Mckay, "A method for registration of 3-D shapes," IEEE Transactions on PAMI, vol. 14, pp. 239–256, February 1992.
3. L. G. Brown, "A survey of image registration techniques," ACM Computing Surveys, vol. 24, no. 4, pp. 325–376, 1992.
4. B. Vemuri and J. Aggarwal, "3-D model construction from multiple views using range and intensity data," in Proc. of IEEE Conference on Computer Vision and Pattern Recognition, pp. 435–437, 1986.
5. P. J. Besl, "The free-form surface matching problem," in Machine Vision for Three-Dimensional Scenes (H. Freeman, ed.), pp. 25–71, New York: Academic Press, 1990.
6. J. B. A. Maintz and M. A. Viergever, "A survey of medical image registration," Medical Image Analysis, vol. 4, no. 1, pp. 1–36, 1998.
7. T. S. Huang, D. B. Goldgof, and H. Lee, "Feature extraction and terrain matching," in Proc. of the IEEE conference on Computer Vision and Pattern Recognition, pp. 899–904, June 1988.
8. Y. Chen and G. Medioni, "Object modelling by registration of multiple range images," Image and Vision Computing, vol. 10, pp. 145–155, April 1992.
9. A. K. Jain, S. Prabhakar, and S. Pankanti, "On the similarity of identical twin fingerprints," Pattern Recognition, vol. 35, no. 8, pp. 2653–2663, 2002.
10. L. O'Gorman, "Fingerprint verification," in Biometrics: Personal Identification in a Networked Society (A. K. Jain, R. Bolle, and S. Pankanti, eds.), pp. 43–64, Kluwer Academic Publishers, 1999.
11. R. L. Graham, "An efficient algorithm for determining the convex hull of a finite planar set," Information Processing Letters, vol. 1, no. 4, pp. 132–133, 1972.
12. A. K. Jain, L. Hong, S. Pankanti, and R. Bolle, "An identity authentication system using fingerprints," Proceedings of the IEEE, vol. 85, no. 9, pp. 1365– 1388, 1997.
13. B. K. P. Horn, "Closed-form solution of absolute orientation using unit quaternions," Journal of the Optical Society of America, vol. 4, pp. 629–642, April 1987.

Article received: 2010-04-21